PERGAMON

International Journal of Solids and Structures 37 (2000) 4125–4147

INTERNATIONAL JOURNAL OF SOLIDS and STRUCTURES

www.elsevier.com/locate/ijsolstr

Experimental studies on the quasi-static axial crushing of steel columns filled with aluminium foam

M. Seitzberger[a,*], F.G. Rammerstorfer[a], R. Gradinger[b], H.P. Degischer[c], M. Blaimschein[d], C. Walch[d]

[a]*Institute of Lightweight Structures and Aerospace Engineering, Vienna University of Technology, Gußhausstraße 27–29, A-1040, Vienna, Austria*

[b]*Centre of Competence on Light Metals, A-5282, Ranshofen, Austria*

[c]*Institute of Materials Science and Testing, Vienna University of Technology, Karlsplatz 13, A-1040, Vienna, Austria*

[d]*VOEST Alpine Stahl Linz GmbH, VOEST-Alpine Straße 3, A-4031, Linz, PO Box 3, Austria*

Received 27 October 1998; in revised form 18 March 1999

Abstract

Experimental investigations are carried out in order to study the effects of different tube and filler arrangements on the crushing behaviour of axially compressed tubular crush elements. To this end quasistatic experiments are performed on monotubal and bitubal, empty and filled steel profiles with different materials, dimensions and cross-sectional shapes. Aluminium foam, produced by a powder metallurgical production process, is applied as filler material. The test results confirm that considerable mass efficiency improvements with respect to energy absorption may be obtained, even if reduced stroke lengths, caused by the presence of foam, are taken into account. Distinct differences are pointed out between the different cross-sectional shapes. Bitubal arrangements, consisting of outer and inner profiles with foam in between, are shown to be particularly efficient crush elements, as long as global failure can be avoided. Explanations for the experimental observations are obtained by a simplified analysis of interaction effects. Constraints concerning the appropriate choice of Al-foam densities are summarized, too, in order to provide an aid for the future design of 'optimally tuned' crush elements composed of tubular members and Al-foam.

Keywords: Axial crushing; Empty profiles; Filled profiles; Aluminium foam; Metal foam

1. Introduction, problem description

In many practical engineering systems there is a requirement for absorbing energy during impact events. Energy absorbers have been developed which dissipate energy in a variety of ways (e.g. by

* Corresponding author. Tel.: +43-1-58801-31719; fax: +43-1-58801-31799.
E-mail address: ms@ilfb.tuwien.ac.at (M. Seitzberger).

0020-7683/00/$ - see front matter
PII: S0020-7683(99)00136-5

friction, fracture, plastic bending or torsion, crushing, cyclic plastic deformation, metal cutting, etc.). Materials used are in general not restricted to metals, but wood, plastics, fiber reinforced polymers and other materials have been applied, too (Jones, 1989).

An ideal energy absorber should be of low weight and maintain the maximum allowable retarding force throughout the greatest possible displacement (stroke length). With respect to these demands the axial compression characteristics of tubular structures that buckle in a progressive manner, can be used to advantage, providing inexpensive and versatile, but nevertheless weight and stroke efficient energy absorbers (Jones, 1989).

In recent years, renewed interest has been observed in the application of cellular structures (honeycombs, foams, etc.) as materials for energy absorption devices. Beside the mass efficiency of such materials their compression characteristics show that they come close to an ideal energy absorber, offering a distinct plateau of almost constant stress in the uniaxial compressive stress-strain curve up to nominal strain values of 70–80% (Gibson and Ashby, 1997; Gradinger et al., 1996; Gradinger, 1997). A number of research groups are currently investigating the mechanical behaviour of cellular materials in order to allow refined predictions of their mechanical properties. At present aluminium foam is of particular practical interest, because efficient and reproducible production routes have been developed in the last years (Banhart, 1997).

With respect to the definition of efficient crush elements, however, a combination of tubular members and cellular filler material seems to be useful, combining synergetically the advantages of both types of structures. The main mechanisms providing enhancements (compared to an empty tube) are the compression of the filler material itself and interaction effects between filler and tube. The interaction leads to higher energy dissipation of the tube due to changed buckling modes (provided that the deformations remain characterized by local modes) and also increases the energy dissipation of the foam core owing to multiaxial compression. A number of authors have contributed to this topic. For example, Reddy and Wall (1988) presented results of static and dynamic tests on very thin circular metal tubes, which were filled with low density polyurethane foam. The presence of the filler material did not only 'stabilize' the almost irregular buckling pattern of the empty cylinders, but also led to efficiency improvements with respect to energy absorption. Reid (1993) reviewed a number of dissipation mechanisms of axially compressed profiles, and described steel tubes filled with polyurethane foam as a particularly efficient energy absorbing device. Seitzberger et al. (1997) have shown experimentally and numerically that filling of square steel tubes with aluminium foam may considerably improve their mass efficiency with respect to the mean forces, provided that the buckling modes of the tubes remain local. Hanssen et al. (1999) also used aluminium foam as filler material to study the influences of filling on the axial crushing behaviour of square aluminium extrusions. In addition to extensive experimental results simple relations between parameters which are likely to influence the crushing behaviour of such composite structures, and design formulas were presented in that work. Santosa and Wierzbicki (1998) used the finite element method for numerically studying filled profiles and also reported on efficiency improvements of axially compressed square aluminium tubes, which were filled with honeycomb or foam. With respect to analytically based numerical methods the extension of the progressive buckling model for prismatic columns, proposed by Abramowicz and Wierzbicki (1989), to cases where foam is used as filler material (Abramowicz and Wierzbicki, 1988) should be mentioned, which, despite its simplicity, allows the consideration of interaction effects between tube and filler.

The intention of the present study is to further contribute to the analysis of specialized tubular 'composite' structures with respect to their energy absorption capacity, when compressed axially at relatively low speeds. To this end tubes made of different grades of steel, having different cross sections (square, hexagonal, octagonal) and dimensions, most of which were filled with aluminium foam, are investigated experimentally. Besides the study of empty and filled tubes ('monotubal' samples), however, special emphasis is laid on crush elements composed of two concentrically oriented profiles with (and

without) aluminium foam in between ('bitubal' crush elements). Such arrangements could offer further mass efficiency improvements with respect to energy absorption and also keep the fluctuation of the resulting axial crushing forces relatively low, owing to both the parallel action of profiles of different dimensions and the influence of the filler material on the buckling modes of the tubular members.

Comparisons with respect to mass efficiency improvements are carried out not only for the mean forces, but also the stroke length and the total energy absorption capacity of the investigated crush elements are considered, which is of major practical interest. Furthermore, an estimation of interaction effects, which are present during crushing of filled elements, is performed in order to give some explanations for the experimental results, but also to obtain conditions for the appropriate choice of tube/filler combinations for the future design of mass efficient crush elements.

2. Experimental setup

2.1. Specimens

The experiments are divided into three groups, in dependence on the material and the tube geometries:

1. Series I: empty and foam filled monotubal square, hexagonal and octagonal profiles, material ZStE340 (these profiles are also used as inner profiles in the bitubal arrangements of series Z).
2. Series S: empty and foam filled square tubes with different arrangements (empty, monotubal filled, bitubal with/without foam in between), material RSt37.
3. Series Z: empty and foam filled tubes with different cross sections (square, hexagonal, octagonal) and varying arrangements (empty, monotubal and bitubal filled), material ZStE340, larger dimensions than series I.

Table 1 gives the dimensions of the investigated tubular members, and in Fig. 1 the arrangements of the bitubal crush elements are sketched. The nomenclature used for describing the tested specimens is as follows. The first letter in the name of each sample refers to the series (I, S, Z), followed by abbreviation letters for the arrangement and/or filling status: E, empty tube(s), i.e. no foam filling used; M, monotubal arrangement; B, bitubal arrangement.

In series I and Z, where different cross-sectional shapes are investigated, the letters are followed by the numbers 4 (square), 6 (hexagonal) and 8 (octagonal), respectively. Each sample designation is finished by a serial number characterizing the specimen. For series S and Z, where bitubal crush elements are also considered, the empty and monotubal members correspond to the outer profiles only.

Table 1
Steel tubes: dimensions (in mm)

	Length l	Thickness t	Mean side length c		
			Square	Hexagon	Octagon
Series I	100	1.5	28.5	20	15
Series S/inner profile	250	1.5	18.5	–	–
Series S/outer profile	250	1.5	38.5	–	–
Series Z/inner profile	250	1.5	28.5	20	15
Series Z/outer profile	250	1.5	64.5	40	30

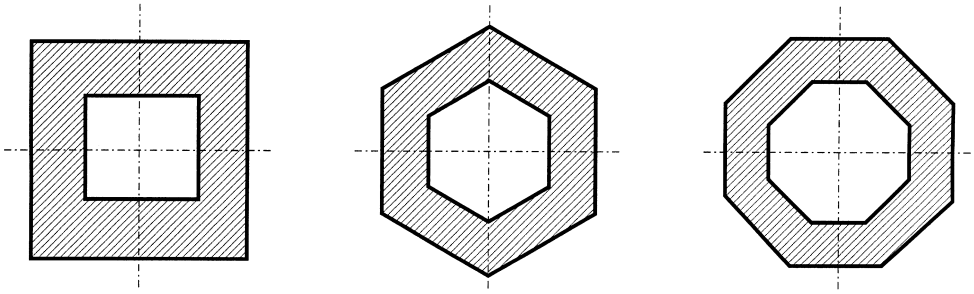

Fig. 1. Bitubal arrangements for square, hexagonal and octagonal cross-sections (series S and Z).

The steel tubes used for series S (material RSt37) were obtained from electrically welded precision profiles, whereas the profiles for series I and Z were manufactured from steel sheets of material ZStE340. The latter is a material that is typically used in automotive engineering. Uniaxial tension test results of both materials are shown in Fig. 2.

The aluminium foam (*Alulight*™) was produced by a powder metallurgical production method, using titanium hydride as foaming agent (Banhart, 1997; Alulight, 1996). Filling of the tubes with foam (base material AlMg0.6Si0.3) was performed in two ways. The profiles of series I and S were foamed directly using the tubes as moulds and in the course of this foaming process the tubes were heated beyond 600°C. Appropriate moulds were used for producing the foam cores for series Z, and consequently these steel tubes were not subjected to such a heat treatment. The influence of this additional heat treatment on the actual material behaviour is shown for RSt37 in Fig. 2, where a distinct annealing effect of the

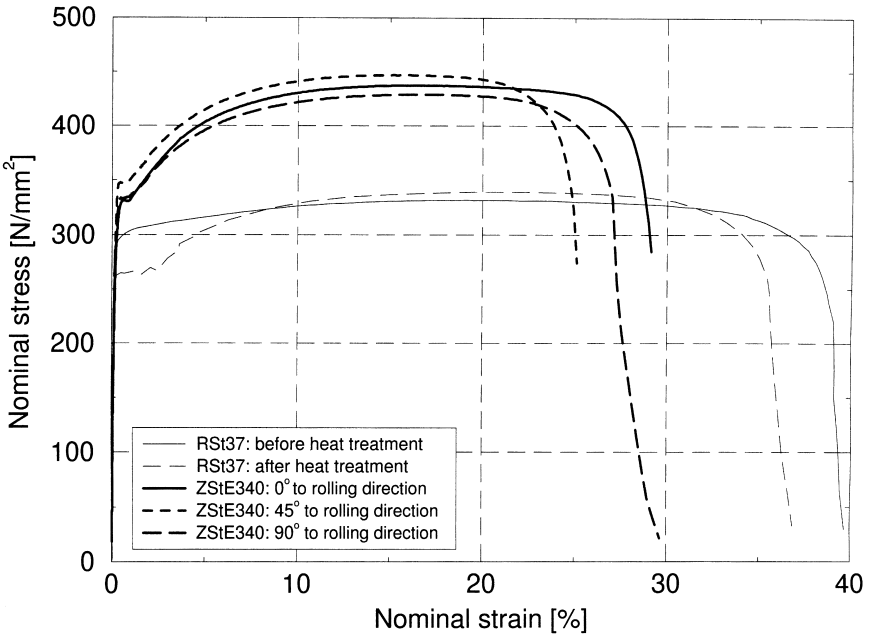

Fig. 2. Material for steel tubes: uniaxial tension test results.

originally cold formed (and therefore strain hardened) tube material can be observed (Seitzberger et al., 1997). In order to obtain comparable results of the crushing process of empty tubes specimens that passed through the same heat treatment as the filled ones were also tested. Except for two samples of series Z the foam cores were not glued to the tubes.

The aluminium foam used for filling the tubes had average densities between 0.37 and 1 g/cm^3. Uniaxial compression test results of the core material (including dense facing material) at different average densities are shown in Fig. 3. In order to obtain these results, actual square core material, which also was used in the monotubal arrangements, was compressed axially at a loading rate of 1 mm/s, which coincides with that used for the crush experiments.

2.2. Experimental details

A universal testing machine was employed for carrying out the experiments. Axial force and crossbeam displacement were recorded digitally using PC based data recording equipment. All samples except the empty bitubal members were tested without special constraints at the ends, i.e. they were compressed axially between two flat plates. For the empty bitubal elements some specialized (distance ensuring) end plates were applied, causing rather fixed boundary conditions for the tubes.

A constant loading velocity of 1 mm/s was used for performing the compression tests. With respect to the deformation behaviour this loading rate can certainly be regarded as quasistatic, i.e. inertia effects will not influence the buckling patterns. Nevertheless, this velocity is sufficiently high to reveal some strain rate sensitivity of the materials of the steel tubes, leading to somewhat elevated force values when compared to static compression tests.

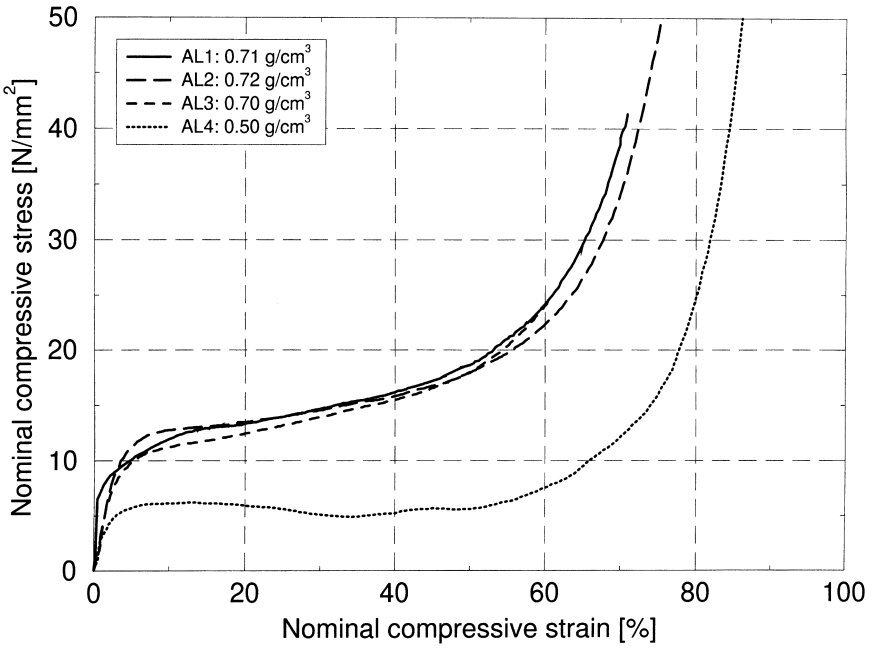

Fig. 3. Aluminium foam (base material AlMg0.6Si0.3) including dense facing material: uniaxial compression test results.

3. Definitions

Before the experimental results are presented and discussed in detail, the variables used are defined and some remarks with respect to these values are given.

- The total mass of a crush element is denoted by m_t.
- ρ_f means the (averaged) apparent density of the aluminium foam.
- F^1_{max} denotes the first load peak, which is associated with first local collapse of the crush element. Due to the strong strain rate sensitivity of the materials, especially with respect to the yield limit, however, this value is expected to be considerably influenced by the chosen loading rate. Therefore, the measured values will be somewhat higher than values which would be obtained with static compression tests. Because the heat treatment, undergone by some specimens, is expected to further affect the measured values (leading to extremely sharp load peaks, as was also reported for RSt37 in (Seitzberger et al., 1997)), however, some uncertainty remains with F^1_{max}.
- s_{max} is the maximum crushing distance. Most experiments were performed up to crushing distances at which the deformation capacity of the tubes is exhausted and/or the densification region of the foam material is reached. This is characterized by a steep increase in the loads exceeding the mean force levels many times. In such cases the force-compression curves are cut at points where the load starts to increase steeply, and so s_{max} coincides with the stroke length s_{st}. Because the definition of this cutoff point is somewhat arbitrary, the given values for the stroke length should be regarded as approximative only. Nevertheless, as the results will show, values obtained for the empty tubes fit theoretical predictions (Abramowicz and Wierzbicki, 1989) quite well, so that the tendencies are thought to come out clearly by the experimental results also for filled tubes.
- Total energy W and mean force F_m are given by

$$W(s) = \int_0^s F(\bar{s})\mathrm{d}\bar{s} \tag{1}$$

and

$$F_m(s) = \frac{W(s)}{s} = \frac{\int_0^s F(\bar{s})\mathrm{d}\bar{s}}{s}, \tag{2}$$

respectively, where F is the applied compressive force and s the crossbeam displacement of the test rig (with integration variable $\bar{s}$). Assuming that the contribution due to elastic deformations is negligible, W can approximately be regarded as the energy dissipated by plastic deformation.
- The stroke efficiency St_e is defined as

$$St_e = \frac{s_{st}}{l}, \tag{3}$$

where s_{st} means the stroke length, and l is the total length of the undeformed crush element (Jones, 1989). The stroke efficiency is (together with the mean crushing force) an important value for estimating the total energy absorption capacity of a given energy absorbing device.
- There are several ways to specify a 'mass efficiency' of a crush element. A rather common measure is the specific energy absorption S_e, which is defined by

$$S_e = \frac{W(s_{st})}{m_t}. \tag{4}$$

The specific energy absorption is a measure for the total energy absorption capacity per unit mass for a given energy absorbing device (Jones, 1989).

In order to allow a direct comparison of the mass related mean force levels of tubular crush elements, which consist of different materials (density ρ_i, cross-sectional area A_i), the quantity

$$S_f = \frac{F_m}{\Sigma \rho_i A_i} \tag{5}$$

is defined. This newly introduced parameter is in the following denoted as 'mean force efficiency'. It can be regarded as the mean force referred to the 'cross-sectional mass', i.e. the mass per unit length of the crush element, $\Sigma \rho_i A_i$. Alternatively, S_f can also be interpreted as the energy which would be absorbed per unit mass if the stroke efficiency were 100%, i.e. if the mean force F_m would act over a crushing distance of length l, which becomes obvious from the following relation:

$$S_e = \frac{W(s_{st})}{m_t} = \frac{F_m(s_{st}) s_{st}}{(\Sigma \rho_i A_i) l} = S_f St_e. \tag{6}$$

Eq. (6) is (with respect to the definitions above) exact only if the stroke length is used for evaluating F_m and S_f, respectively. If, however, quasi-steady deformation processes (like the progressive buckling of tubes) are considered, the mean force is approximately constant over s (oscillating only slightly around a constant value with decreasing amplitude). Hence, $F_m(s)$ with s sufficiently large, but smaller than the stroke length, can be used, too.

Concerning the description of experimentally observed failure modes distinctions are made between global (G) and local failure mechanisms (where, with respect to the bitubal members only the deformations of the outer, because visible, profiles are considered). The local deformation behaviour is furthermore described by:

I: inextensional folding modes, where the individual lobes around the circumference of the tubular

Fig. 4. Series S: empty and monotubal crushed specimens SEM2, SM13 ($\rho_f = 0.43$ g/cm^3), SM15 ($\rho_f = 0.68$ g/cm^3).

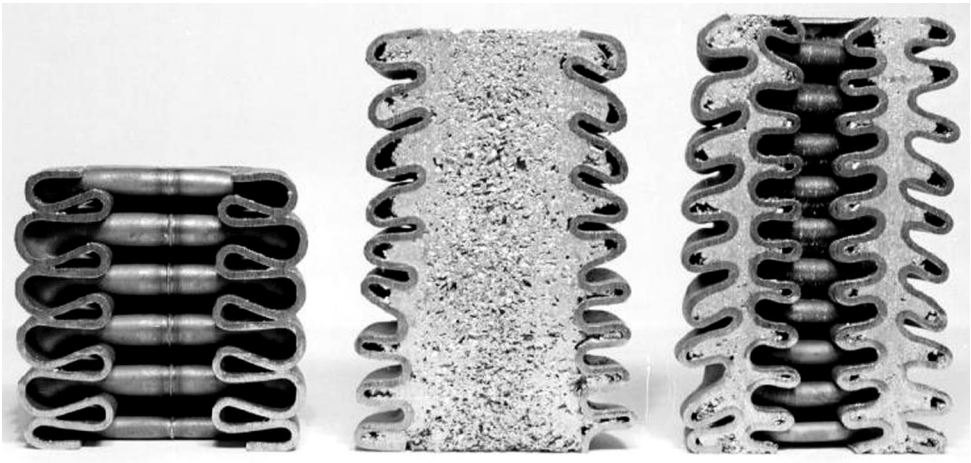

Fig. 5. Series S: sections of samples SEM1, SM13 ($\rho_f = 0.43$ g/cm^3), SB19 ($\rho_f = 0.59$ g/cm^3).

members alternatively move inwards and outwards, this way avoiding large hoop strains (see e.g. the empty square tubes in Figs. 4 and 5);

E: extensional folding modes with all lobes moving outwards (accompanied by large hoop strains and more pronounced load peaks in the axial force-compression curves, see e.g. the monotubal filled octagonal member in Fig. 6);

P: progressive buckling, i.e. the sequential formation of adjacent local folding patterns (typical samples are shown in Figs. 4 and 5);

L: local, but not typically progressive buckling (irregular folding, irregular progressive buckling, see e.g. sample ZB85 in Fig. 7);

W: breaking of the welding seams.

Fig. 6. Series Z: square, hexagonal and octagonal monotubal crushed specimens ZM44 ($\rho_f = 0.47$ g/cm^3), ZM64 ($\rho_f = 0.47$ g/cm^3), ZM83 ($\rho_f = 0.58$ g/cm^3).

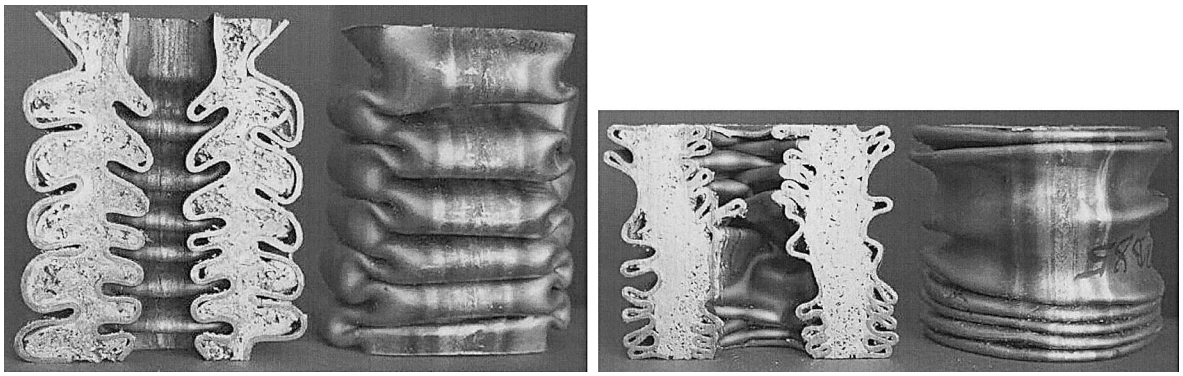

Fig. 7. Series Z: sections of samples ZB45 ($\rho_f = 0.58$ g/cm^3, glued), ZB85 ($\rho_f = 0.66$ g/cm^3).

4. Summary of test results

4.1. Experimental observations

Photographs of some crushed specimens (including sectioned samples) can be seen in Figs. 4–7 and typical measured force-compression curves of the different test series are shown in Figs. 8–12. Table 2 includes a listing of the measured and evaluated test results, according to the definitions above. Table 2, in addition, contains a description concerning the failure modes observed during the experiments as well as remarks with respect to the preparation of the individual samples.

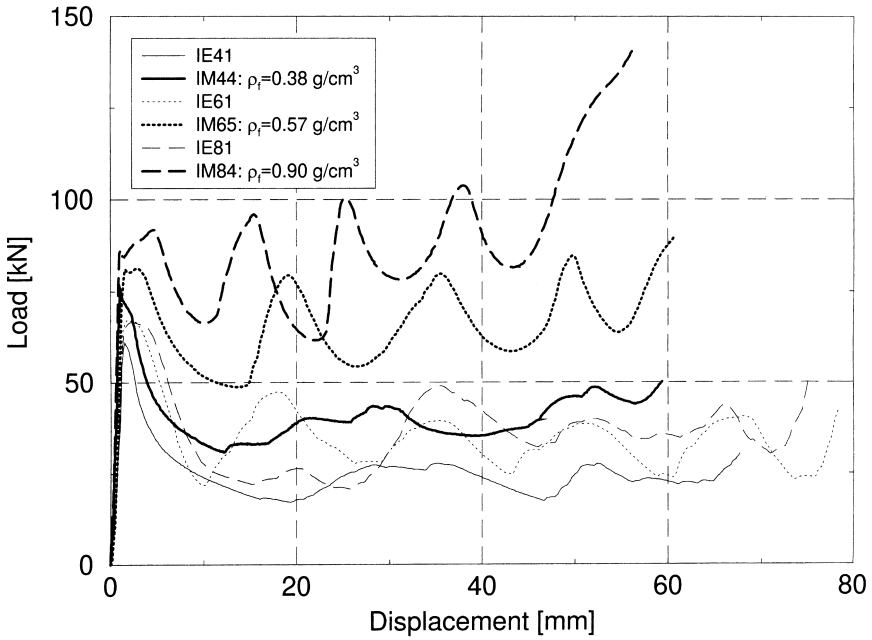

Fig. 8. Series I: typical load versus compression curves.

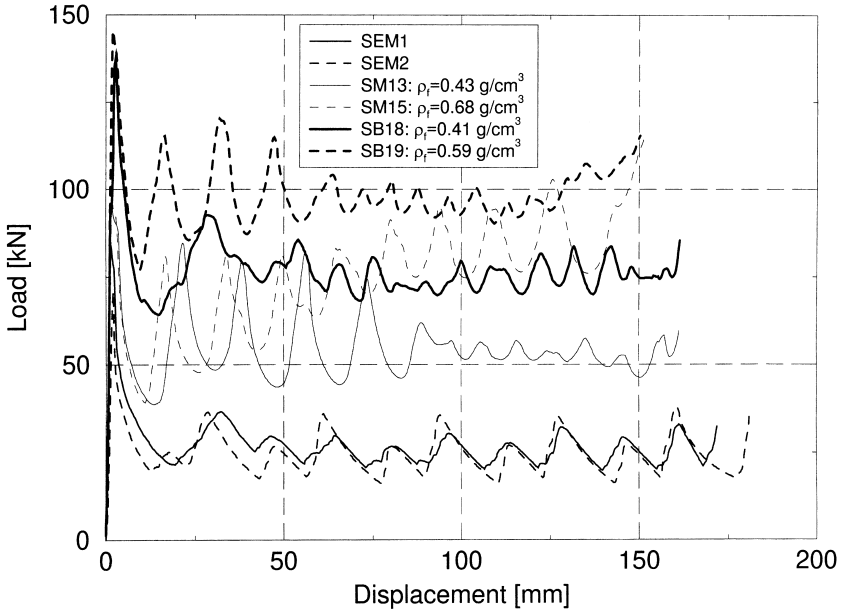

Fig. 9. Series S: typical load versus compression curves.

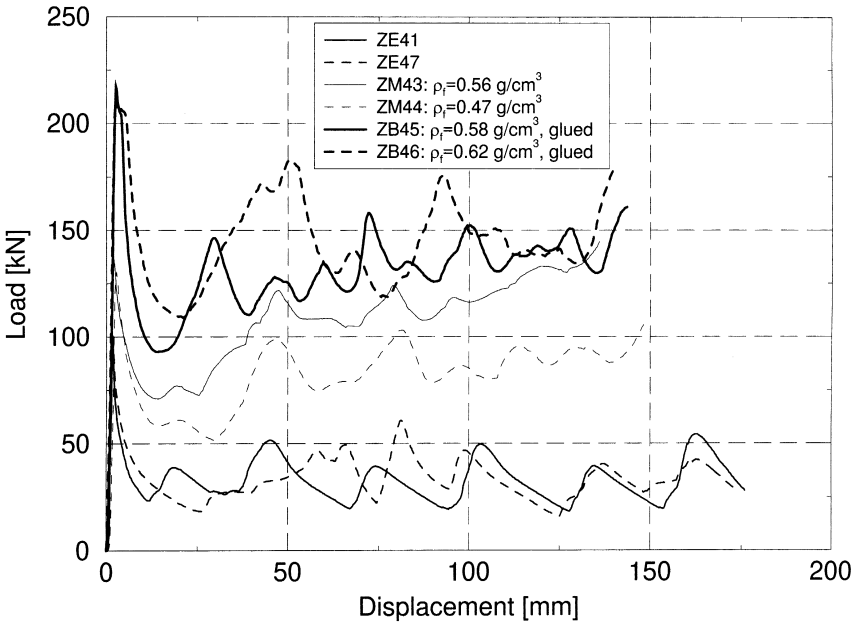

Fig. 10. Series Z, square cross-sections: typical load versus compression curves.

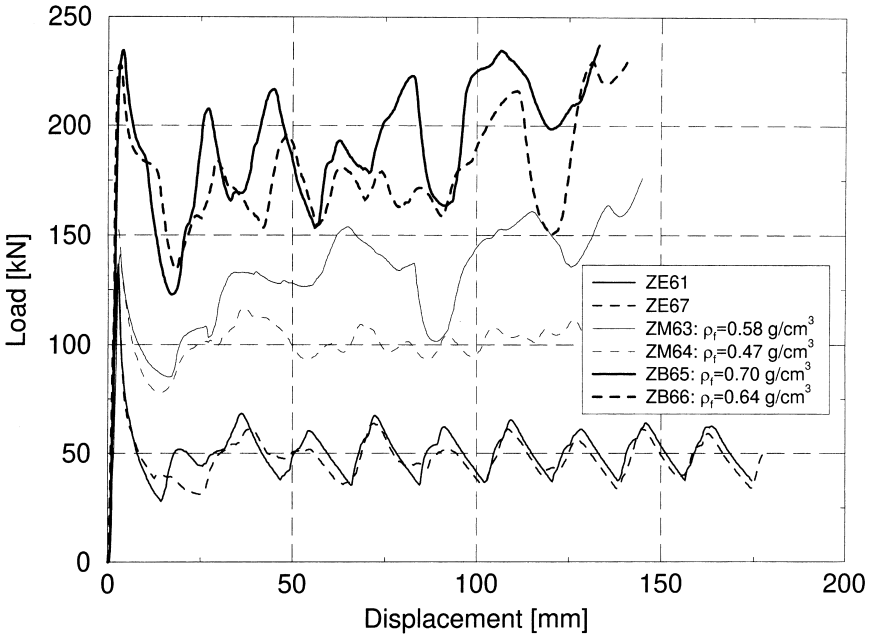

Fig. 11. Series Z, hexagonal cross-sections: typical load versus compression curves.

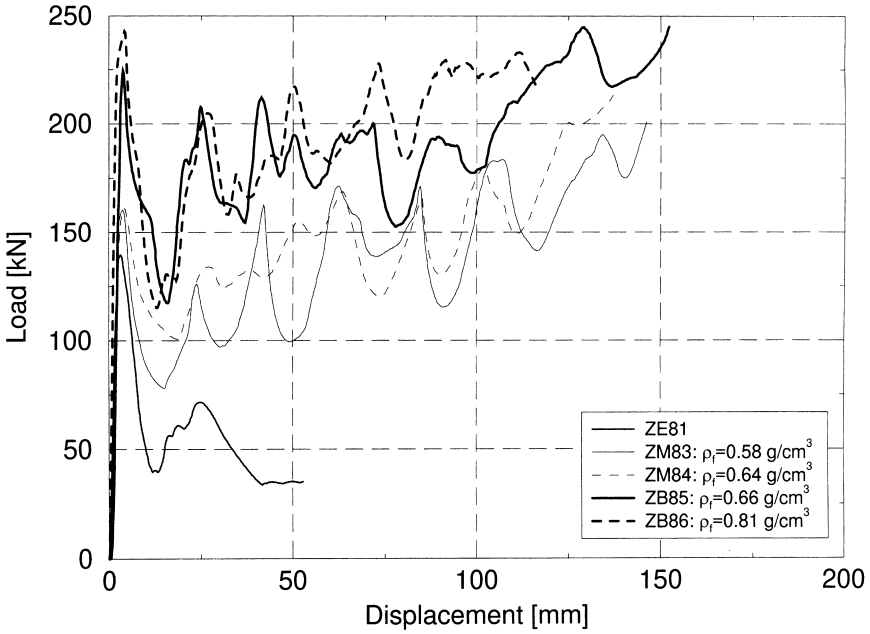

Fig. 12. Series Z, octagonal cross-sections: typical load versus compression curves.

Table 2
Test results

Sample	m_t [g]	ρ_f [g/cm^3]	F^1_{max} [kN]	s^a_{max} [mm]	$W(s_{max})$ [kJ]	$F_m(s_{max})$ [kN]	St_e[a] [%]	S_f [kJ/kg]	S_e [kJ/kg]	Failure mode[b]	Remarks[c]
Series I											
IE41	124	Empty	61.0	68	1.67	24.7	68	19.9	13.5	P	
IE42	126	Empty	71.2	73	2.45	33.5	73	26.6	19.4	P	No ht
IE43	125	Empty	71.6	73	2.50	34.2	73	27.4	20.0	L	No ht
IM44	153	0.38	75.3	59	2.41	40.6	59	26.5	15.8	P	
IM45	160	0.47	74.7	63	2.81	44.9	63	28.1	17.6	P	
IE61	138	Empty	67.2	78	2.73	34.7	78	25.1	19.8	P	
IE62	141	Empty	84.9	45	1.66	36.9	–	26.2	–	L-G	No ht
IE63	140	Empty	81.1	75	3.32	44.2	75	31.6	23.7	L	No ht
IM65	194	0.57	81.4	61	3.99	65.6	61	33.8	20.6	L(E)	
IM67	231	0.96	88.4	55	4.64	84.3	55	36.5	20.1	L(E)	
IE81	138	Empty	66.7	75	2.68	35.7	75	25.9	19.4	P(E)-L	
IE82	139	Empty	81.4	74	2.98	40.3	74	29.0	21.4	L	No ht
IE83	139	Empty	79.7	75	2.68	35.5	75	25.5	19.3	L	No ht
IM84	229	0.90	91.9	56	4.96	88.4	56	38.6	21.7	L(E)	
IM85	238	1.00	89.3	51	4.60	89.9	51	37.8	19.3	L(E)	
Series S											
SEM1	438	Empty	84.0	172	4.66	27.1	69	15.5	10.6	P	
SEM2	437	Empty	70.9	181	4.50	24.8	72	14.2	10.3	P	
SM12	611	0.50	93.7	157	9.41	59.9	63	24.5	15.4	P(E-I)	
SM13	588	0.43	96.7	161	8.83	54.8	64	23.3	15.0	P(E-I)	
SM14	605	0.48	95.7	157	9.07	57.7	63	23.8	15.0	P(E3-I)	
SM15	672	0.68	97.0	152	11.36	75.0	61	27.9	16.9	P(E-I)	
SM16	566	0.37	96.9	167	7.52	45.1	67	19.9	13.3	P(E-I)	
SEB6	660	Empty	119.8	50	2.77	55.9	–	21.2	–	P-G	
SB17	768	0.45	144.3	163	13.43	82.4	65	26.8	17.5	P(E-I)	
SB18	758	0.41	137.7	161	12.37	76.7	64	25.3	16.3	P(E-I)	
SB19	803	0.59	145.4	150	14.73	98.1	60	30.5	18.3	P(E-I)	
SB20	775	0.48	143.4	–	–	–	–	–	–	L-G	
SB21	773	0.47	149.1	–	–	–	–	–	–	L-G	
Series Z											
ZE41	734	Empty	97.9	176	5.85	33.2	–	11.3	–	P	No ht
ZE47	734	Empty	102.2	174	5.93	34.0	–	11.6	–	L-P	No ht
ZE48	734	Empty	106.9	166	5.51	33.1	–	11.3	–	L	No ht
ZM43	1290	0.56	136.3	136	14.7	108.1	54	20.9	11.4	L	No ht
ZM44	1204	0.47	130.3	148	12.1	81.7	59	17.0	10.0	L-P	No ht
ZB45	1561	0.58	217.2	143	18.8	130.7	57	20.9	12.0	P	No ht, g
ZB46	1579	0.62	211.3	140	20.2	144.4	56	22.9	12.8	L	No ht, g
ZE61	709	Empty	136.7	175	8.92	51.1	–	18.0	–	P	No ht
ZE67	709	Empty	132.3	178	8.62	48.4	–	17.1	–	P,W	No ht
ZE68	709	Empty	136.2	158	8.08	51.1	–	18.0	–	L,W	No ht
ZM63	1284	0.58	140.8	145	19.0	131.1	58	25.5	14.8	L(E),W	No ht
ZM64	1178	0.47	152.9	146	14.7	101.2	58	21.5	12.5	P	No ht
ZB65	1554	0.70	234.4	133	25.3	190.3	53	30.6	16.3	L	No ht
ZB66	1515	0.64	227.8	141	25.1	178.0	56	29.4	16.6	L	No ht
ZE81	709	Empty	139.5	–	–	–	–	–	–	L-G	No ht
ZE87	709	Empty	134.7	–	–	–	–	–	–	L-W-G	No ht
ZE88	709	Empty	137.7	–	–	–	–	–	–	L-W-G	No ht
ZM83	1319	0.58	160.3	146	20.3	138.9	58	26.3	15.4	P(E)	No ht
ZM84	1377	0.64	161.1	137	20.1	146.9	55	26.7	14.6	P-L	No ht
ZB85	1552	0.66	224.4	152	28.9	190.0	61	30.6	18.6	P(E)-L,W	No ht
ZB86	1663	0.81	242.8	116	22.4	193.4	–	29.1	–	P(E)-W	No ht

[a] If a value is given for St_e, then s_{max} means stroke length.

[b] P, progressive buckling; L, local, but not progressive buckling; E, extensional folding mode (E3 ... 3 folds moving outwards); G, global failure.

[c] No ht, steel tubes did not pass through a heat treatment analogous to that occurring during foaming the filler material; g, glued.

With respect to the failure modes of test series I (monotubal empty and filled square, hexagonal and octagonal profiles with small cross-sectional dimensions) the experiments revealed that progressive buckling could almost exclusively be observed for some empty tubes and the filled crush elements with square cross-sections (Table 2). All hexagonal and octagonal filled profiles of this test series (having a higher foam density than the square ones) rather showed local, but not typically progressive, deformation behaviour, where the formation of folds began at different locations, generally not in a sequential manner. Furthermore, these specimens buckled extensionally (with all folds moving outwards), which is obviously caused by the presence of the foam core. The extensional deformations are also evident from the force-compression curves (Fig. 8), because the load fluctuations are much more pronounced. Filling of the tubes was in general accompanied by shorter wavelengths of the individual folds (which holds true for all test series).

Within test series S empty and foam filled square tubes, which were arranged in different ways (empty, monotubal filled, bitubal with and without filler material), were tested. The material used for the steel profiles, RSt37, is different from that used in the other two test series. The typical progressive buckling characteristics, which could be observed in most experiments of this test series, are evident from the deformed elements shown in Figs. 4 and 5. The monotubal filled sample in Fig. 5 also reveals the higher densification in the outer region of the foam core due to a multiaxial state of compression (resulting from foundation effects of the foam with respect to the profile). Global failure was observed only for the bitubal empty and some of the bitubal foam filled elements. This can be traced back to global buckling of the slender inner profiles, leading to overall buckling of the whole arrangements. All filled specimens that deformed locally began to buckle in an extensional mode, but after the formation of some folds most switched to an inextensional mode, which is typical for the empty profiles of this type (see Fig. 4). The measured force-compression curves (Fig. 9) also clearly display the effects of the change of deformation modes. The filled specimens show a pronounced load fluctuation during the first load cycles, owing to the extensional folding modes, which is followed by minor differences between maximum and minimum loads due to the inextensional buckling deformations of the steel tubes. Furthermore, the force-compression curves reveal a distinct quasi-steady progress of the crushing forces (fluctuating around a more or less constant value), provided that the average foam density is not too high. The ascending slope of the force level of sample SM15 (seen in Fig. 9), however, is due to the foam behaviour itself. The stress-strain curves of uniaxially compressed foam cores shown in Fig. 3 indicate that for foams of higher densities no marked plateau region (characterized by more or less constant stresses), but rather a region of constantly increasing stresses can be observed (Gradinger, 1997), thus corresponding with the measured force-compression behaviour of crush elements filled with foams of higher densities.

The third group of tests, series Z, includes uniaxial compression tests on empty as well as on monotubal and bitubal filled tubular crush elements with varying cross sectional shapes (square, hexagonal and octagonal) and larger dimensions than those of series I. Some typical deformed specimens of monotubal filled elements are shown in Fig. 6, and Fig. 7 includes photographs of the sectioned bitubal members ZB45 and ZB85 (note that sample ZB85 was crushed far beyond the stroke length). Whereas the square and hexagonal specimens rather tended to buckle inextensionally, a typical extensional folding mode is apparent from the octagonal crush elements of this test series. Furthermore, many of the investigated elements started with the simultaneous formation of folds at different locations, and as a result a local, but not typically progressive buckling behaviour could be observed (see e.g. sample ZB85 in Fig. 7). For the empty octagonal specimens this led, in combination with breaking of the welding seams, to global buckling of the tubes. The gluing between filler and tubes of samples ZB45 and ZB46 obviously caused the lobes to be filled with aluminium foam for the most part (left side of Fig. 7). However, some breaking of the interface can also be observed for these samples. It should be noted, however, that the main reason for applying adhesive for these specimens was to fix the foam core

and the tubes prior to testing and not to provide a perfect interface for higher energy absorption purposes.

Force-compression curves for the different cross-sectional shapes of test series Z are presented in Figs. 10–12. The curves for the square and hexagonal empty profiles show a more or less repeated load-displacement pattern, characteristic for progressive buckling. Whereas a very regular curve with low load fluctuations was also measured for sample ZM64 ($\rho_f = 0.47$ g/cm^3, Fig. 11), the other foam filled specimens, mostly having a somewhat higher filler density, do not reveal such a smooth behaviour. This can be traced to the failure modes described above, i.e. the occurrence of irregular progressive buckling, extensional folding modes and/or fracture of the welding seams. In addition, the bitubal arrangements may buckle in a manner that local load maxima or minima belonging to outer and inner profiles occur simultaneously, thus also delivering distinct load extrema for the whole composite structure.

4.2. Efficiency considerations

The results obtained for the different efficiency parameters, which are listed in Table 2, are presented for all three test series in graphical form in Figs. 13–15, in dependence on the average density of the filler material (except those empty specimens of test series I, that did not pass through a heat treatment analogous to that occurring during foaming of the filler material). In order to indicate the tendencies, linear fits (if appropriate) are included in the diagrams, too.

For the empty square and hexagonal profiles of test series Z, where testing was stopped shortly before the axial compression capacity was exhausted ($s_{max}/l \approx 70\%$), a stroke efficiency of 0.73 was assumed (proposed by Abramowicz and Wierzbicki (1989) for square tubes) and also used for the evaluation of the specific energy absorption S_e of these profiles, included in Fig. 15 (by applying Eq. (6)).

4.2.1. Stroke efficiency

Fig. 13 shows a distinct decrease of the measured stroke efficiencies St_e with increasing foam density. The measured stroke efficiencies of 68–78% for the empty tubes (fitting the theoretical value of 0.73 quite well) are reduced to values of 50–60% for higher foam densities, with some differences within and between the individual test series. The reduction of the stroke efficiencies can certainly be traced back to the foam behaviour. With increasing foam density the region of densification, i.e. the region, where the compressive force starts to increase steeply, is shifted to lower values of the compressive strain. For example, the stroke efficiencies of the measured (uniaxially compressed) foam cores, which are shown in Fig. 3, lie at about 60% for an apparent foam density of 0.7 g/cm^3, whereas with 0.5 g/cm^3 a value of more than 70% can be observed. Furthermore, it must be expected that during the formation of the folds some foam material is trapped within the folds (see e.g. Figs. 5 and 7). This material will suffer very large compressive strains and may prevent the folds from touching each other, this way also reducing the resulting stroke length of the whole crush element. Hanssen et al. (1999), who did experimental work on square aluminium extrusions filled with Hydro aluminium foam, obtained a similar reduction of the stroke efficiencies. For preliminary design purposes a lower bound of 55% was suggested for St_e (coinciding with the results presented here).

4.2.2. Mean force efficiency

Regarding the mean force efficiency S_f, distinct enhancements due to foam filling are shown in Fig. 14 for all investigated crush elements. The filled tubes of test series I deliver improvements of up to 40–50% for all cross-sectional shapes (however, for different foam densities), and the monotubal square specimens of test series S and Z offer maximum improvements of more than 80% (!), as compared to the empty profiles of the same types. Even higher absolute values for S_f can be observed for the corresponding bitubal crush elements, mainly owing to the higher mean force efficiencies of the inner

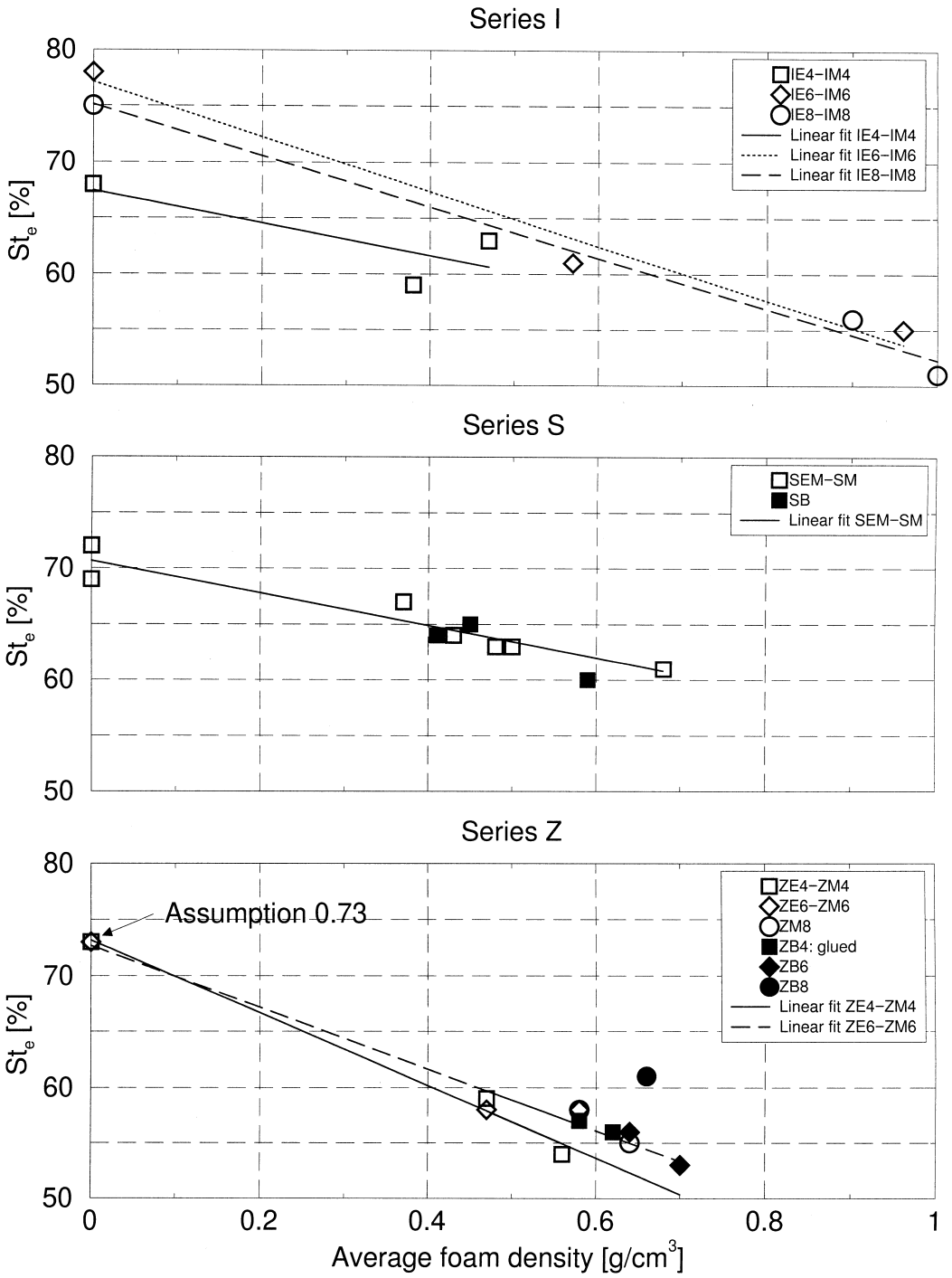

Fig. 13. Stroke efficiency versus density diagram.

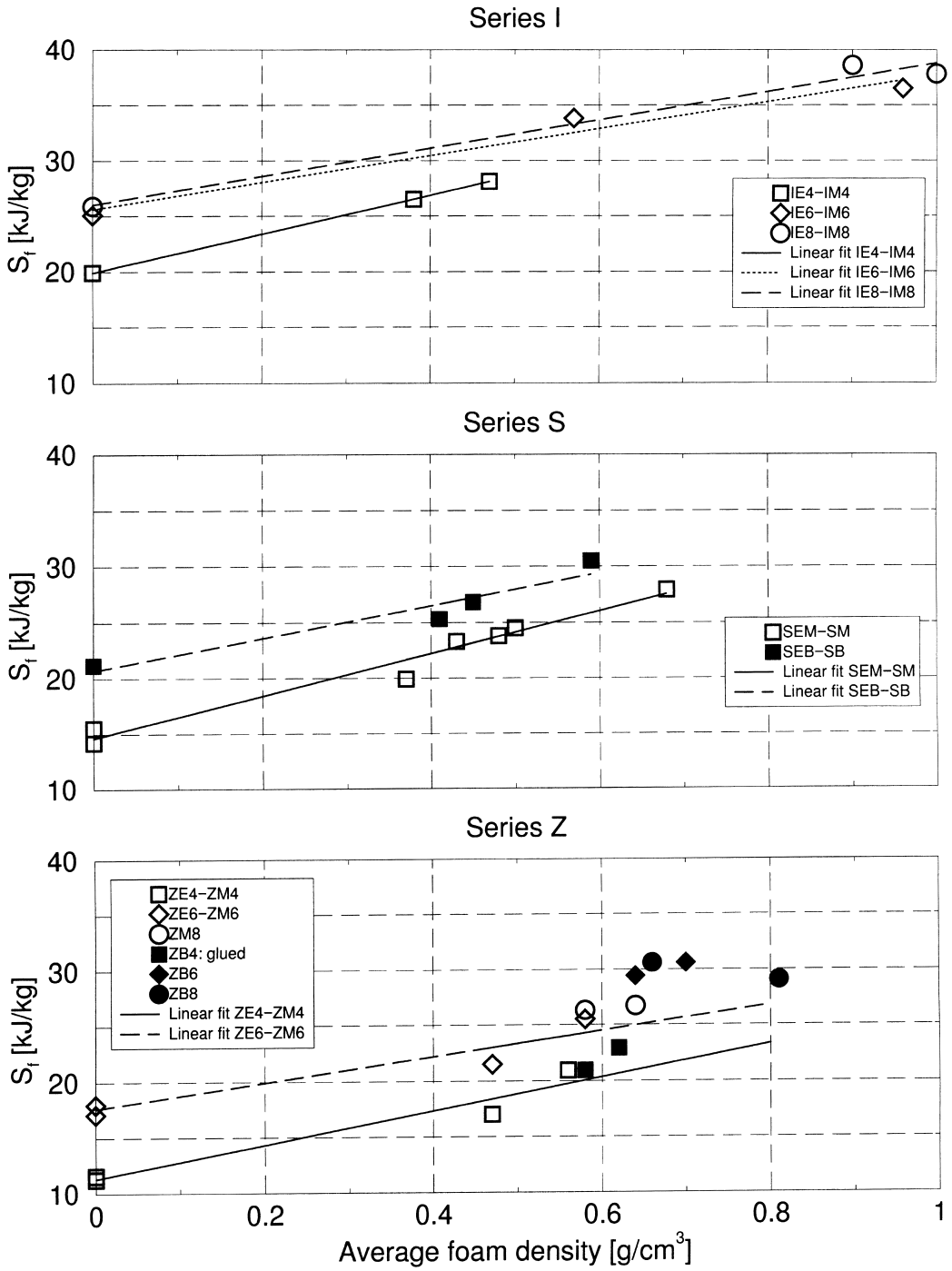

Fig. 14. Mean force efficiency versus density diagram.

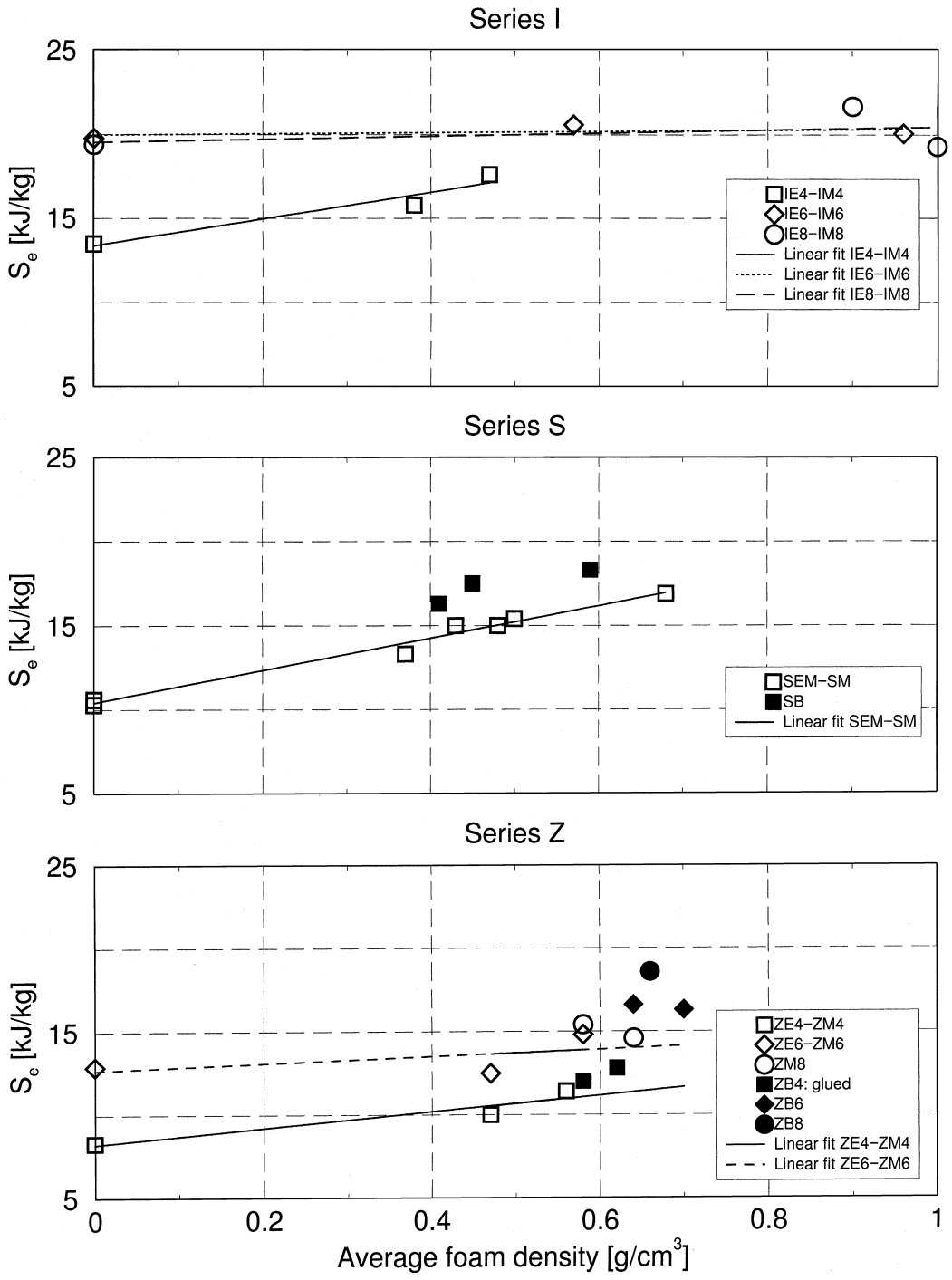

Fig. 15. Specific energy absorption versus density diagram.

profiles themselves. This is not only indicated by higher values for the empty profiles of test series I, as compared to series Z, but can also be seen from a comparison between empty monotubal and bitubal arrangements of series S (for a more detailed discussion of these effects see Section 5). However, the 'sensitivity' with respect to global failure, i.e. beam-type buckling of one of the tubes, must also be taken into account for these crush elements. If the enhancements are to be utilized, the tube dimensions have to be selected carefully in order to avoid some critical slenderness of the inner profile.

The relative increase of S_f of the monotubal hexagonal members of series Z is not as pronounced as that of the square specimens. Nevertheless, distinct increases of the mean force efficiency of more than 40% could be measured. The octagonal specimens (where all empty tubes failed globally) seem to be comparable to the hexagonal crush elements. The absolute values for the bitubal arrangements of these cross-sectional shapes once again exceed those of the monotubal ones to some extent.

4.2.3. Specific energy absorption

A comparison of the energy absorption capacity of the crush elements with respect to the total mass, S_e, can be seen in Fig. 15. Due to a decrease of the stroke efficiency, St_e, with increasing foam densities ($S_e = S_f St_e$, see Eq. (6)), the enhancements for S_e are certainly lower than those observed for S_f. Nevertheless, marked improvements could be measured for all arrangements with square cross-sectional shapes. The maximum relative increases of the monotubal square crush elements are between 30% (test series I and Z) and 60% (test series S), where average foam densities between 0.5 and 0.7 g/cm^3 have been applied. However, the test results on the hexagonal and octagonal arrangements within test series I do not reveal any marked enhancements of S_e with increasing foam density, and also for the larger cross-sectional dimensions of test series Z only slight improvements can be observed.

The results for those bitubal arrangements that buckled locally still markedly lie above those of the tested monotubal crush elements, indicating the potential of such specialized crush elements for energy absorption devices.

5. Discussion of results

5.1. Cross-sectional shapes and dimensions

A result attracting attention in Figs. 14 and 15 is that hexagonal and octagonal members are obviously markedly more efficient than square ones. This behaviour can be traced back to the crushing behaviour of the empty profiles itself. Theoretical analyses (Wierzbicki and Abramowicz, 1989) predict that (empty) hexagonal cross-sections are able to resist considerably higher mean axial stresses than square ones. A comparison of the hexagonal and octagonal specimens of test series I, however, delivers similar results for the mean force values, indicating no marked preferences for one of these cross-sectional shapes.

With respect to the different cross-sectional dimensions, markedly higher mean force efficiencies become obvious for test series I (having smaller dimensions), if compared to series Z. This is due to the fact that an essential part of the energy dissipation comes from deformations in the corner regions, whereas the contribution of the deformations due to bending of the lobes is not as pronounced (Abramowicz and Wierzbicki, 1989). An increase of the side lengths of the tubular members, therefore, increases the cross-sections of the specimens, but does not enlarge the crushing forces by a comparable amount. The mean force efficiency enhancements of the bitubal arrangements may, to a great extent, also be traced back to the higher mean force efficiencies of the inner profiles.

5.2. Interaction effects

For estimating interaction effects the mean crushing force of an axially compressed composite crush element, F_m, may be divided into several additive components (Santosa and Wierzbicki, 1998; Hanssen et al., 1999):

$$F_m = \Sigma F_{m,\,i} + F_{m,\,int}, \tag{7}$$

where $F_{m,i}$ are the mean crushing forces, which are obtained if the individual members (empty profiles, foam core) are compressed axially, and $F_{m,int}$ denotes the contribution to F_m resulting from interaction effects. Eq. (7) may alternatively be written in terms of the mean force efficiency S_f. Dividing by m_t/l $(=\Sigma\rho_i A_i)$ gives

$$S_f = \Sigma\frac{m_i}{m_t}S_{f,\,i} + S_{f,\,int}\ (\rightarrow S_{f,\,int} = S_f - \Sigma\frac{m_i}{m_t}S_{f,\,i}), \tag{8}$$

where m_i is the mass of constituent i $(m_t=\Sigma m_i)$, and $S_{f,i}$ and $S_{f,int}$ are given as $F_{m,i}l/m_i$ and $F_{m,int}l/m_t$, respectively. The interaction term mainly comprises increases of F_m (and S_f, respectively) due to changed buckling modes of the tube(s) and multiaxial (instead of uniaxial) compression of the foam. Therefore, it generally depends on the chosen geometry and on both the tube and the foam material behaviour.

Measured values for the nonfilled profiles are available from the test results. However, a suitable description of the foam material behaviour is also needed in order to allow an estimation of $S_{f,int}$ according to Eq. (8). In (Gradinger, 1997) results of an experimental study on uniaxially compressed aluminium foams are presented, including the Al-foams used here. For the mean force efficiency $S_{f,f}$ of an uniaxially compressed foam core (base material AlMg0.6Si0.3, without dense facing material) curve fitting of the test results gives the dimension dependent relation ($S_{f,f}$ in kJ/kg, ρ_f in g/cm^3):

$$S_{f,\,f} = 21.54\rho_f^{0.63}. \tag{9}$$

This relation was obtained for test samples having an average foam density between 0.2 and 0.9 g/cm^3, which were loaded quasistatically. However, because the evaluation points for obtaining Eq. (9) were chosen somewhat conservatively (the corresponding nominal compressive strains, which depend on ρ_f, are below 50%), it may slightly underestimate the actual mean force efficiencies of the foam cores of the crush elements (which were subjected to higher axial compressive strains), but will certainly be sufficient to reveal tendencies.

The results of the estimation of $S_{f,int}$ for the tested mono- and bitubal crush elements are presented in graphical form in Fig. 16, and Fig. 17 shows the relative influences of interaction effects on the total mean force efficiencies, $S_{f,int}/S_f$ (which coincide with the mean force ratios $F_{m,int}/F_m$), both as functions of the average foam density. These estimates show that interaction effects contribute essentially to the energy dissipation of the investigated crush elements, provided the foam densities are chosen high enough. A distinct increase of the influences of interaction effects can be seen at lower foam densities. Above 0.5–0.6 g/cm^3 maximum relative influences are reached, where the higher values correspond to the monotubal filled square tubes (Fig. 17). The results for series S furthermore show that both the absolute values and the relative influences of the bitubal members (SB) are markedly lower than those of the monotubal ones (SM). This coincides with the experimental observations, as can be seen in Fig. 14 for test series S, where the dependence of the bitubal crush elements on foam filling seems to be lower than that of the monotubal members (according to the lower slope of the corresponding curve fit).

Furthermore, marked differences can be observed for the different cross-sectional dimensions, with the smaller tubes activating higher interaction effects per unit mass than the larger ones (compare test series

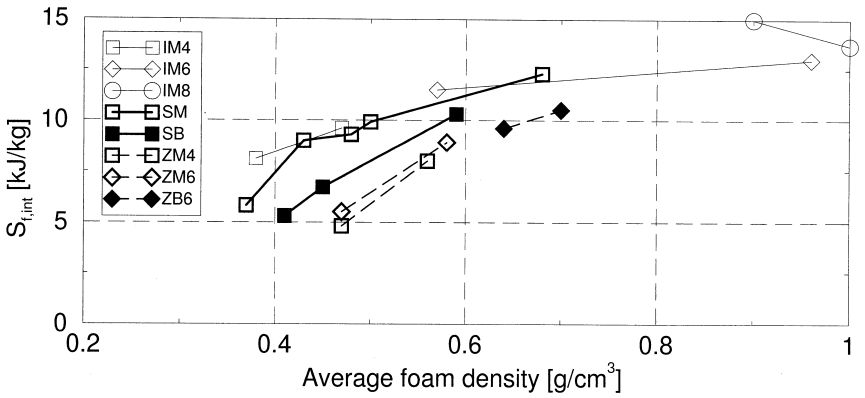

Fig. 16. Mean force efficiency due to interaction effects versus density diagram.

I and Z in Fig. 16). However, a rather surprising outcome of these estimations is that the influences of the cross-sectional shapes seem not to be pronounced. Dependent on the average foam density comparable interaction effects are activated for the different monotubal cross-sectional shapes with test series I and Z, as can be seen from Fig. 16.

The considerations and results presented in this section, however, allow for some simplified explanation of the experimental observations mentioned above. Consider the parallel action of two constituents 1 and 2 (e.g. tube and foam or outer and inner profile, respectively) without activating any

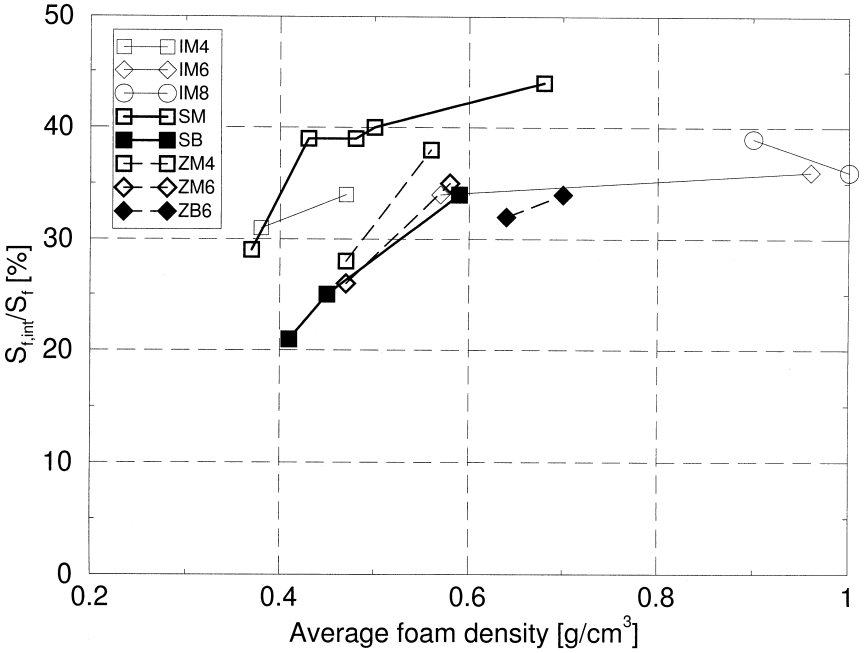

Fig. 17. Interaction effects on the mean force efficiency: relative influence versus density diagram.

interaction effects. Then, Eq. (8) is written as

$$S_f = \frac{m_1}{m_1+m_2} S_{f,\,1} + \frac{m_2}{m_1+m_2} S_{f,\,2} = S_{f,\,1} + \frac{m_2}{m_1+m_2}(S_{f,\,2} - S_{f,\,1}). \tag{10}$$

From this equation it follows that, depending on the mass ratios, the resulting mean force efficiency S_f always lies within $S_{f,1}$ and $S_{f,2}$. Consequently, constituent 1 can only be improved if $S_{f,2}$ is larger than $S_{f,1}$. Because the inner profile of a bitubal arrangement in general is more efficient than the outer one, the total mean force efficiency of an empty bitubal member already exceeds that of the outer profile (but reduces that of the inner one). With respect to the design of filled crush elements these simple considerations show that the mean force efficiency of a tubular member should not exceed that of the foam material too much. Even if (additional) interaction effects are activated, the efficient tube behaviour may in the worst case deteriorate as a consequence of filling!

Relative improvements with respect to constituent 1 (now including an interaction term) are given by

$$\frac{S_f}{S_{f,\,1}} = \frac{m_1}{m_1+m_2} + \frac{1}{S_{f,\,1}}\left(\frac{m_2}{m_1+m_2} S_{f,\,2} + S_{f,\,\mathrm{int}}\right). \tag{11}$$

Provided, only the mean force efficiency of constituent 1 changes, then it follows from Eq. (11) that the higher the value for $S_{f,1}$ the lower relative improvements are. This, however, is approximately given within the individual test series (having comparable mass ratios). Consider a monotubal filled specimen with constituent 1 being the tubular member and constituent 2 the foam core. $S_{f,f}(=S_{f,2})$ is a pure function of the foam densities, and also the activation of interaction effects is (for a given foam density) seen to be comparable for the different cross-sectional shapes (Fig. 16). Thus square tubes, themselves being less efficient than hexagonal or octagonal members, yield the highest relative efficiency improvements, confirming the experimental results for test series I and Z.

With respect to the activation of interaction effects, it furthermore seems reasonable, that the mean force efficiencies of the constituents should in general not differ too much, because otherwise one member is expected to dominate the other, this way eventually inducing minor interaction effects.

6. Filled crush elements—design considerations

The number of investigated samples as well as the number of different test series are (without further theoretical analyses) certainly not sufficient to propose definite design formulas. However, the test results are appropriate to reveal basic constraints, which are important for the design of (unbonded) filled crush elements. These design constraints may be divided into conditions coming from the behaviour of the individual members (foam, tubes) and from the combination of these constituents in order to synergetically evoke interaction effects.

Besides the appropriate choice of foam material (i.e. metallic or organic foams, which is not discussed here) the main parameter for the foam core is its apparent mass density. From the uniaxial compression behaviour of aluminium foam, (Fig. 3, (Gradinger, 1997)), it may be learned that higher foam densities result in:

- the densification region being shifted to lower compressive strain values;
- the distinct plateau region rather becoming a region of monotonically increasing stresses.

Both items directly influence the behaviour of the investigated crush elements in a negative way. Therefore, an upper bound for the foam density can be given, which essentially depends on the foam material! For example, for the investigated samples a maximum value of 0.5–0.6 g/cm^3 seems to be appropriate.

With respect to the combination of tube and foam to build up mass efficient energy absorption devices it has to be taken into account that

- the mean force efficiencies of the constituents should not differ too much—a lower mean force efficiency for the tubular member will be advantageous (see the discussion in Section 5.2);
- a higher foam density leads to:
  - an increased tendency for the (outer) tubes to buckle extensionally,
  - an increased tendency towards global failure,
  - but also to the activation of higher interaction effects!

With respect to the last point it was shown in Section 5.2 (Figs. 16 and 17) that for the investigated crush elements the average foam density should at least be 0.3–0.4 g/cm^3 in order to evoke substantial interaction effects and efficiency improvements, respectively.

As a result, for the tested samples apparent foam densities of 0.3–0.5(0.6) g/cm^3 might be 'optimal' for obtaining a regular progressive buckling behaviour, dominated by inextensional folding modes and, hence, with not too large load-fluctuations, while retaining marked efficiency improvements with respect to the mean forces. Because the stroke efficiency should also remain high for such densities, distinct improvements of the whole specific energy absorption capacity can be expected. To our experience this does not only apply to monotubal crush elements with square cross-section (although the improvements are most pronounced in this case), but also to hexagonal cross-sections and bitubal arrangements. If bitubal arrangements are chosen, the cross-sectional dimensions have to be selected carefully in order to avoid global failure of one of the tubes. Such composite structures are, therefore, expected to be of advantage mainly in structures that have to resist considerable compressive forces, so that larger cross-sectional dimensions have to be applied in any case.

7. Summary and conclusions

The test results presented here confirm that the mass related mean force level may considerably be improved by filling tubular members with aluminium foam. Provided that the plastic buckling behaviour remains characterized by local modes, essential enhancements were obtained for all investigated shapes and dimensions. These improvements may partly be traced back to the axial compression of the foam cores themselves, but interaction effects also play a substantial role (simple estimates have shown that for the investigated configurations up to more than a third of the total mean forces results from interaction effects between tubes and foam cores). With respect to the total energy absorption capacity of a given crush element, however, improvements are less pronounced. The reason for this is that the maximal crushing distances, which may be utilized for energy dissipation, reduce with increasing foam densities. Nevertheless, improvements of the mass specific energy absorption of monotubal square members of up to 60% were obtained, revealing the large potential offered by such composite crush elements!

Distinct differences have been pointed out between the different cross-sectional shapes, where (for similar cross-sectional areas) square profiles are shown to be preferable to hexagonal and octagonal tubes, as far as improvement by filling is concerned. These, however, may also be improved markedly, if suitable tube/filler combinations are chosen. The tendencies towards extensional buckling modes, which are in general accompanied by larger load fluctuations, are also shown to increase with increasing foam densities and hexagonal as well as octagonal members.

The investigation of bitubal arrangements revealed that these may be preferable to monotubal specimens. It could be shown that improvements are mainly due to the presence of the inner profiles,

which are in general more mass efficient than the outer ones. Interaction effects are somewhat less pronounced that for monotubal tubes.

An analysis of interaction effects was performed, which not only allowed to determine the relative influences of such effects onto the mean force levels but also to find some explanations concerning the differences between cross-sectional shapes and mono- and bitubal arrangements, respectively. Furthermore, some basic conditions for the appropriate choice of tube/filler combinations could be obtained this way.

Design considerations, pointing out the essential constraints for the appropriate choice of foam densities for the construction of mass efficient crush elements, have been summarized. However, all considerations stated therein are restricted to quasistatic loading conditions. Future testing will be required to investigate the behaviour of dynamically loaded crush elements, which are filled with aluminium foam. Furthermore, influences of gluing have to be investigated in more detail, because they are expected to markedly influence the energy absorption capacity of filled crush elements. With respect to the design of 'optimally tuned' composite crush elements, numerical methods could also turn to account, which allow to gain more insight into the mechanics of such (complex) plastic deformation processes, too.

Acknowledgements

The financial support of the work by the Austrian 'Fonds zur Förderung der wissenschaftlichen Forschung (FWF)', contract number P12092-MAT, and the provision of the facilities for compression tests by the Institute for Testing and Research in Materials Technology (TVFA), Vienna University of Technology, are gratefully acknowledged.

References

Abramowicz, W., Wierzbicki, T., 1988. Axial crushing of foam-filled columns. Int. J. Mech. Sci. 30 (3/4), 263–271.

Abramowicz, W., Wierzbicki, T., 1989. Axial crushing of multicorner sheet metal columns. J. Appl. Mech. 56, 113–120.

Alulight, 1996. 'Alulight'—material description. MEPURA, A-5282 Ranshofen.

Banhart, J., 1997. Metallschäume, Proceedings of Symposium Metallschäume. 6–7 March, 1997, Bremen, Verlag MIT, Bremen.

Gibson, L.J., Ashby, M.F., 1997. Cellular Solids: Structure and Properties, 2nd ed. Cambridge University Press, Cambridge, New York, Melbourne.

Gradinger, R.C., 1997. Das mechanische Verhalten von Aluminsiumschaum bei Druck- und Crushbelastung—Experimente und numerische Simulation. Diploma thesis, Vienna University of Technology, Vienna.

Gradinger, R.C., Kretz, R., Degischer, H.P., Rammerstorfer, F.G., 1996. Deformation behaviour of aluminium foam under compressive loading. In: Proceedings of JUNIOR-EUROMAT, 26–30 August 1996, Lausanne, Switzerland.

Hanssen, A.G., Langseth, M., Hopperstad, O.S., 1999. Static crushing of square aluminium extrusions with aluminium foam filler. Int. J. Mech. Sci. 41, 967–993.

Jones, N., 1989. Structural Impact. Cambridge University Press, Cambridge, UK.

Reddy, T.Y., Wall, R.J., 1988. Axial compression of foam-filled thin-walled circular tubes. Int. J. Impact. Eng. 7 (2), 151–166.

Reid, S.R., 1993. Plastic deformation mechanisms in axially compressed metal tubes used as impact energy absorbers. Int. J. Mech. Sci. 35 (12), 1035–1052.

Santosa, S., Wierzbicki, T., 1998. Crush behavior of box columns filled with aluminium honeycomb or foam. Computers and Structures 68 (4), 343–367.

Seitzberger, M., Rammerstorfer, R.F., Degischer, H.P., Gradinger, R., 1997. Crushing of axially compressed steel tubes filled with aluminium foam. Acta Mechanica 125, 93–105.

Wierzbicki, T., Abramowicz, W., 1989. The mechanics of deep plastic collapse of thin-walled structures. In: Wierzbicki, T., Jones, N. (Eds.), Structural Failure. Wiley, New York, pp. 281–329.